Environmental Pollution 342 (2024) 123092

Contents lists available at ScienceDirect

Environmental Pollution

journal homepage: www.elsevier.com/locate/envpol

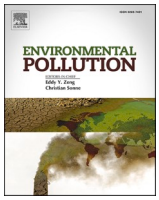

Non-regulated haloaromatic water disinfection byproducts act as endocrine and lipid disrupters in human placental cells☆

Elisabet Pérez-Albaladejo [a], Marta Casado [a], Cristina Postigo [b,c], Cinta Porte [a,*]

[a] Environmental Chemistry Department, IDAEA -CSIC-, C/ Jordi Girona, 18-26, 08034, Barcelona, Spain
[b] Technologies for Water Management and Treatment Research Group, Department of Civil Engineering, University of Granada, Avda Severo Ochoa s/n, Campus de Fuentenueva, Granada, 18071, Spain
[c] Institute for Water Research (IdA), University of Granada, Ramón y Cajal 4, 18071, Granada, Spain

ARTICLE INFO

Keywords:
Halobenzoquinones
Water disinfection
Reprotoxicity
Micronuclei
Oxidative stress

ABSTRACT

The disinfection of drinking water generates hundreds of disinfection byproducts (DBPs), including haloaromatic DBPs. These haloaromatic DBPs are suspected to be more toxic than haloaliphatic ones, and they are currently not regulated. This work investigates their toxicity and ability to interfere with estrogen synthesis in human placental JEG-3 cells, and their genotoxic potential in human alveolar A549 cells. Among the haloaromatic DBPs studied, halobenzoquinones (2,6-dichloro-1,4-benzoquinone (DCBQ) and 2,6-dibromo-1,4-benzoquinone (DBBQ)) showed the highest cytotoxicity (EC_{50}: 18–26 μg/mL). They induced the generation of very high levels of reactive oxygen species (ROS) and up-regulated the expression of genes involved in estrogen synthesis (*cyp19a1*, *hsd17b1*). Increased ROS was linked to significant depletion of polyunsaturated lipid species from inner cell membranes. The other DBPs tested showed low or no significant cytotoxicity ($EC_{50} \geq 100$ μg/mL), while 2,4,6-trichloro-phenol (TCP), 2,4,6-tribromo-phenol (TBP) and 3,5-dibromo-4-hydroxybenzaldehyde (DCHB) induced the formation of micronuclei at concentrations much higher than those typically found in water (100 μg/mL). This study reveals the different modes of action of haloaromatic DBPs, and highlights the toxic potential of halobenzoquinones, which had a significant impact on the expression of placenta steroid metabolism related genes and induce oxidative stress, implying potential adverse health effects.

1. Introduction

The use of chlorine for water disinfection has been a valuable resource to eliminate waterborne diseases. However, the interaction of chlorine with the organic matter and the inorganic ions (e.g., bromide, iodide) present in water results in the unintended formation of a wide spectrum of disinfection byproducts (DBPs) (e.g., haloacetic acids, trihalomethanes, nitrosamines, haloacetonitriles, haloacetamides, and haloaromatic compounds, among others) (Richardson and Postigo, 2015). Exposure to many of these DBPs is a cause of concern due to their adverse effects in human health (Richardson et al., 2007). In this regard, DBP exposure has been associated with increased incidence of bladder cancer, miscarriage, and developmental effects in epidemiological studies (Grellier et al., 2015; Villanueva et al., 2014).

Haloaromatic DBPs in chlorinated water are formed by the reaction of chlorine with aromatic compounds (e.g. phenols, hydroxybenzoic acids) present in the humic fraction of natural organic matter (NOM). During chlorination, these aromatic structures may release from NOM and be the target of electrophilic halogenation (Jiang et al., 2020). Haloaromatic DBPs further decompose into aliphatic ones, such as haloacetic acids (HAAs) and trihalomethanes (THMs), although detailed data on stability of aromatic DBPs is lacking (Liu et al., 2020). Haloaromatic DBPs have been frequently detected in chlorinated tap water at the ng/L level; however, they are rarely quantitatively determined because of the complexity of their analysis and the lack of analytical standards for many of them (Hu et al., 2018; Lou et al., 2021b; Tao et al., 2020; Zhang et al., 2019, 2018; 2020). The haloaromatic fraction constitutes about 30% of the total organic halogenated material found in chlorinated water (Han et al., 2021). However, its toxicity has been scarcely addressed, even though they are suspected to be more toxic than haloaliphatic DPBs (Liu and Zhang, 2014). In fact, several studies have shown that the overall toxicity of chlorinated water samples is often dominated by aromatic halo-DBP fractions, probably due to their

☆ This paper has been recommended for acceptance by Wen Chen.

* Corresponding author.
E-mail address: cpvqam@cid.csic.es (C. Porte).

https://doi.org/10.1016/j.envpol.2023.123092
Received 25 October 2023; Received in revised form 27 November 2023; Accepted 1 December 2023
Available online 9 December 2023

List of acronyms

AB	Alamar Blue
CE	Cholesterol ester
Cer	Ceramide
CFDA-AM	5-carboxyfluorescein diacetate acetoxymethyl ester
cyp19a1	Cytochrome P450 family 19 subfamily A member 1
DBBQ	2,6-dibromo-1,4-benzoquinone
DBHB	3,5-dibromo-4-hydroxybenzaldehyde
DBHBA	3,5-dibromo-4-hydroxybenzoic acid
DBPs	Disinfection by products
DBSA	3,5-dibromo-salicylic acid
DCBQ	2,6-dichloro-1,4-benzoquinone
DCHB	3,5-dichloro-4-hydroxybenzaldehyde
DCHBA	3,5-dichloro-4-hydroxybenzoic acid
DCSA	3,5-dichloro-salicylic acid
DG	Diacylglycerols
DMEM	Dulbecco's Modified Eagle Medium
DMSO	Dimethyl sulfoxide
DPBS	Phosphate buffered saline with Ca and Mg
FBS	Fetal bovine serum
gapdh	Glyceraldehyde-3-phosphate dehydrogenase
H_2DCF-DA	2′,7′-dichlorodihydrofluorescein diacetate
hsd17b1	Hydroxysteroid 17-beta dehydrogenase 1
hsd17b12	Hydroxysteroid 17-beta dehydrogenase 12
hsd3b1	Hydroxy-delta-5-steroid dehydrogenase, 3 beta- and steroid delta-isomerase 1
LPC	Lyso - phosphatidylcholine
LPE	Lyso - phosphatidylethanolamine
MEM	Eagle's Minimum Essential Medium
PBS	Phosphate-buffered saline
PC	Phosphatidylcholines
PC-O	Phosphatidylcholine -plasmanyl
PC-P	Phosphatidylcholine -plasmalogen
PE	Phosphatidylethanolamines
PE-O	Phosphatidylethanolamine -plasmanyl
PE-P	Phosphatidylethanolamine -plasmalogen
PI	Phosphatidylinositol
PLS-DA	Partial least square - discriminant analysis
PS	Phosphatidylserine
ROS	Reactive oxygen species
RSD	Relative standard deviation
SIN-1	3-morphoolinosydnonimine
SM	Sphingomyelin
TBP	2,4,6-tribromophenol
TCP	2,4,6-trichlorophenol
TG	Triacylglycerols
VIP	Variable influence on the projection

considerably higher potential to bioconcentrate and generate reactive oxygen species in the organism (Liu et al., 2020; Wang et al., 2018). When considering the toxicity of haloaromatic DBPs, it is noteworthy that, similar to haloaliphatic DBPs, it tends to decrease in the order iodinated > brominated ≫ chlorinated compounds (Liu et al., 2020). Although for benzoquinones, higher toxicity has been reported for chlorinated compounds compared to brominated ones (Li et al., 2015).

As for the toxicity of the various haloaromatic DBP classes, extensive research has been conducted on halobenzoquinones. 2,6-Dichloro-1,4-benzoquinone (DCBQ) demonstrated significant cytotoxicity and generation of reactive oxygen species (ROS) in human colon and liver cancer cells (Hung et al., 2019). Additionally, halobenzoquinones exerted neurotoxicity by inducing cell cycle arrest in human neural stem cells (hNCS) (Fu et al., 2017). Besides, their genotoxic and carcinogenic potential is supported by the ability of their transformation byproducts (hydroxybenzoquinones) to cause DNA damage (Li et al., 2015). Similarly, halobenzoquinones showed developmental toxicity manifested as malformations in zebrafish larvae, heart malformations, curved spines, and failed inflation of the gas bladder, which was partially attributed to increased ROS production (Wang et al., 2018). Quinone-induced oxidative stress resulted in oxidative damage to proteins and DNA, leading to the formation of DNA adducts, and possibly the oxidation of lipids, although the latter has not been investigated in depth (Du et al., 2014).

Understanding the mode of action for DBPs is still needed, particularly for adverse developmental effects, like spontaneous abortion, low birth weight or cardiovascular malformations, often related to DBP exposure (Colman et al., 2011). Non animal models (NAMs) based on the use of specific cell lines can generate valuable information on the mode of action of chemicals and include dose-response studies. For instance, the use of human placental cells revealed that bromodichloromethane inhibited the secretion of human chorionic gonadotropin (hCG) in trophoblast cells at concentrations in the range of those reported in human blood (0.082 μg/L) (Chen et al., 2004). In another study, haloacetic acids decreased the expression of the steroidogenic gene *hsd17b1* involved in the synthesis of estradiol in JEG-3 placental cells (Pérez-Albaladejo et al., 2023). Placental cells retain a functional estrogen receptor and the mechanisms for regulating the expression of genes involved in steroidogenesis. This characteristic renders them an ideal model to investigate the endocrine disruption potential of exogenous compounds (Karahoda et al., 2021). As for genotoxicity, the human alveolar cell line A549 is a good model to detect micronucleus formation during mitosis, as a consequence of DNA damage. This cell line has shown good sensitivity to exposure to haloacetic acids, among other pollutants (Barillet et al., 2010; Pérez-Albaladejo et al., 2023). Moreover, alveolar cells, by their nature, are of relevance to assess the toxicity of volatile and semi-volatile DBPs. Inhalation of less volatile DBPs, such as haloacetic acids, may be a relevant exposure pathway in specific environments where they present high concentrations in the gas phase (e.g., indoor areas intensively disinfected (Lou et al., 2021a) or indoor swimming pools (Yang et al., 2018)).

In this context, this work aimed at increasing the knowledge on the toxicological potential of haloaromatic DBPs. Built upon previous studies, our hypothesis was that haloaromatic DBPs would exhibit reprotoxic and genotoxic properties in human cells, and that some of them, particularly halobenzoquinones, would induce oxidative stress. To test this hypothesis, ten chlorinated and brominated analogues belonging to five different chemical classes, namely benzoquinone, hydroxybenzaldehyde, benzoic acid, salicylic acid, and phenol were selected (Table S1). Their toxicity, and ability to induce the generation of ROS, and regulate the expression of genes involved in the metabolism of steroids in placenta was determined in JEG-3 cells, while their genotoxic potential was assessed in A549 lung cells. Emphasis was placed on exploring the lipidome of JEG-3 cells following exposure to halobenzoquinones to assess potential effects on lipid oxidation and/or disregulation of lipid metabolism. This work applies for the first time a lipidomic approach to explore the reprotoxic modes of action of halobenzoquinones in human placental cells.

2. Material and methods

2.1. Chemicals and reagents

Eagle's Minimum Essential Medium (MEM), L-glutamine, sodium pyruvate, nonessential amino acids, penicillin and streptomycin, phosphate buffered saline with Ca and Mg (DPBS), and trypsin-EDTA 0.25 %

were from Gibco BRL Life Technologies (Paisley, UK). Dulbecco's Modified Eagle Medium (DMEM), fetal bovine serum (FBS), 2′,7′-dichlorodihydrofluorescein diacetate (H_2DCF-DA), bisbenzimide 33342 Hoechst, and dimethyl sulfoxide (DMSO) were from Merck (Darmstadt, Germany). Alamar Blue (AB), 5-carboxyfluorescein diacetate acetoxymethyl ester (CFDA-AM), and 3-morphoolinosydnonimine (SIN-1) were obtained from Invitrogen (Paisley, UK). High purity analytical standards (>97 %) of the selected haloaromatic DBPs were obtained from Merck (2,6-dichloro-1,4-benzoquinone (DCBQ), 3,5-dichloro-4-hydroxybenzaldehyde (DCHB), 3,5-dibromo-4-hydroxybenzaldehyde (DBHB), 3,5-dichloro-4-hydroxybenzoic acid (DCHBA), 3,5-dichloro-salicylic acid (DCSA), 3,5-dibromo-salicylic acid (DBSA), 2,4,6-trichlorophenol (TCP), 2,4,6-tribromophenol (TBP)) and Carbosynth (Compton, UK) (2,6-dibromo-1,4-benzoquinone (DBBQ) and 3,5-dibromo-4-hydroxybenzoic acid (DBHBA)) (Table S1).

2.2. Cell culture

Human placental choriocarcinoma JEG-3 cells (ATCC HTB-36) were routinely grown in MEM supplemented with 5 % FBS, 1 mM sodium pyruvate, 2 mM L-glutamine, 0.1 mM nonessential amino acids, 1.5 g/L sodium bicarbonate, 50 U/mL penicillin and 50 μg/mL streptomycin. Human alveolar carcinoma A549 cells (ATCC CCL-185) were maintained in DMEM supplemented with 10 % FBS, 4 mM L-glutamine, 50 U/mL penicillin and 50 μg/mL streptomycin. Both, JEG-3 and A549 cells were incubated at 37 °C and 5 % CO_2 in a humidified incubator. When 90 % confluence was reached, cells were dissociated with 0.25 % trypsin-EDTA for subculturing and experiments.

2.3. Analysis of cell viability

JEG-3 cells were plated at a density of 4×10^4 cells per well in a 96-plate well (Nunclon Delta Surface, Thermo, Roskilde, Denmark), incubated overnight and exposed for 24 h to different concentrations of the selected haloaromatic DBPs or 0.1 % DMSO (solvent control). After washing with phosphate-buffered saline (PBS), cells were incubated for 60 min in a solution of 5 % Alamar Blue (AB) and 4 μM CFDA-AM in mineral medium (Leibovitz L-15/ex). The fluorescence of AB and CFDA-AM were measured in a Tecan Infinite M Plex plate reader (Männedorf, Switzerland) at the excitation/emission wavelengths of 530/590 and 485/530 nm, respectively. Cell viability was expressed as a percentage of the fluorescence measured in solvent control cells.

2.4. Reactive oxygen species (ROS)

The ability of haloaromatic DBPs to induce the production of ROS in JEG-3 cells was investigated using H_2DCF-DA as a substrate, as described in Pérez-Albaladejo et al. (2023). JEG-3 cells seeded in 96-well plates (4×10^4 cells/well) were washed with PBS and incubated for 30 min in a solution of 20 μM H_2DCF-DA. After removing this solution, cells were exposed to different concentrations of DBPs, 5 μM SIN-1 (positive control) or 0.1% DMSO (solvent control). The fluorescence was read after 15, 30, 60 and 120 min of exposure at the excitation/emission wavelengths of 485/528 nm in a Tecan Infinite M Plex reader. ROS production was expressed as a percentage of the fluorescence measured in solvent control cells. Three independent experiments were performed in different days, and six replicates per plate were analyzed.

2.5. Analysis of gene expression

JEG-3 cells were plated in 6-well culture plates (10^6 cells/well) and exposed for 24 h to 5 μg/mL of DBPs in a final concentration of 0.1% DMSO. RNA isolation was carried out with TRIzol™ (Invitrogen Life Technologies, Carlberg, Denmark). The purity and quantity of the RNA were determined using a NanoDrop™ 8000 spectrophotometer (Thermo Scientific). The obtained RNA (5 μg) was treated with DNase I (Ambion, Austin, TX, USA) as described in Pérez-Albaladejo et al. (2023). Taqman Gene Expression Assays (Applied Biosystems, Thermo Fisher Scientific, Inc) were used to quantify the expression levels of *cyp19a1* (cytochrome P450 family 19 subfamily A member 1), *hsd3b1* (hydroxy-delta-5-steroid dehydrogenase, 3 beta- and steroid delta-isomerase 1); *hsd17b1* (hydroxysteroid 17-beta dehydrogenase 1); *hsd17b12* (hydroxysteroid 17-beta dehydrogenase 12); and *gapdh* (glyceraldehyde-3-phosphate dehydrogenase, used as the reference gene). The relative mRNA abundance of each gene was calculated using the $2^{-\Delta\Delta Cp}$ method (Livak and Schmittgen, 2001).

2.6. Micronuclei formation in A549 cells

Cells were seeded in 6-well plates (1.5×10^5 cells/well in 2 mL DMEM) containing 3 glass coverslips (Ø 12 mm; Marienfeld, Germany) as described in Pérez-Albaladejo et al. (2023). Cells were exposed to non-toxic concentrations of DBPs for 48 h, 0.25 μM mitomycin C (positive control) or 0.1 % DMSO (solvent control). After exposure, cells were washed, fixed with 4 % formaldehyde for 30 min, and stained with 5 μM bisbenzimide (Hoechst 33342). Then, the coverslips were mounted with Vectashield H-1000 (Vector Laboratories, CA, USA). Images of each coverslip were obtained with an EVOS M7000 Cell Imaging System (Thermo Fisher Scientific). Individual images were taken in an area of the coverslip in the automated mode with autofocus; the images were then tiled and exported to Celleste 5.0 Image Analysis Software for the automatic counting of the nuclei. Micronuclei were manually counted on individual images following the criteria described in Fenech (2000).

2.7. Analysis of lipids

JEG-3 cells were seeded in 24-well plates (10^5 cells/well), and after 24-h attachment, they were exposed to 0.5, 1 and 5 μg/mL of selected haloaromatic DBPs (DBBQ and DCBQ), or 0.1 % DMSO (solvent control). The haloaromatic DBPs and exposure concentration for lipid analysis were selected based on the high levels of ROS induction observed for these compounds. After 24 h of exposure, cell pellets were collected and stored at −80 °C as described in Pérez-Albaladejo et al. (2019). Lipids were extracted with ethyl acetate (500 μL); the mixture was vortexed for 1 min, incubated for 30 min at room temperature, and ultrasound-extracted for 5 min and the supernatant collected. This extraction cycle was repeated twice. The solvent was evaporated under a gentle stream of N_2 and the extracts were stored under argon atmosphere at −80 °C. Flow injection analysis of reconstituted lipid extracts was conducted in an Orbitrap-Exactive mass spectrometer (Thermo Fisher Scientific) as described in (Pérez-Albaladejo et al., 2019). These analyses were done using a constant flow rate (50 μL/min) of methanol: dichloromethane (80:20, v/v) and full scan mass acquisition (m/z 200–2000) and in positive (ESI+) and negative (ESI-) electrospray ionization modes. The duration of the analytical run was 2 min. Mass spectra were processed using Xcalibur 2.1 (Thermo Fisher Scientific, Bremen, Germany) and the lipid species were quantified (pmol/10^5 cells) relative to internal standards. Based on the MS response observed for the internal standard mixture, only sodium adducts [M + Na+] were considered for ESI+, and single negatively charged ions [M-H] in ESI^-. Mass peaks considered in ESI + corresponded to triacylglycerols (TG), diacylglycerols (DG), phosphatidylcholines (PC), PC-plasmanyl [PC-O]/PC- plasmalogen [PC-P]. In ESI-, phosphatidylethanolamines [PE], PE-plasmanyl [PE-O]/PE-plasmalogen [PE-P], phosphatidylserines [PS], and phosphatidylinositol [PI] were identified. The internal standards used in the quantification process included 16:0D31–18:1 phosphatidylcholine, 17:0 lyso-phosphatidylcholine, 15:0–18:1D7 diacylglycerol, 1,2,3–17:0 triacylglycerol, 16:0D31 sphingomyelin, 16:0D31 ceramide, 16:0D31–18:1 phosphatidylethanolamine, 16:0D31–18:1 phosphatidylserine, and 16:0D31–18:1 phosphatidylinositol (Avanti Polar Lipids, Inc., Alabama, USA). The relative standard

deviation (RSD) of the internal standards through the analytical batch ranged from 17 % to 30 % except for 1,2,3–17:0 triacylglycerol, which was comparatively higher (43 %). RSD of 10 no consecutives injections of external standards was satisfactory ranging from 8 % (PC) to 21 % (PS).

2.8. Statistical analysis

Dose-response curves and concentrations causing 50 % decline on cell viability (EC_{50}) were calculated with Sigmaplot 13.0. Significant differences from controls were determined using one-way ANOVA with Dunnett's post-hoc test using SPSS Statistics 27.0. Level of significance was set at $p < 0.05$. Lipid profiles were analyzed using Metaboanalyst 5.0 (Pang et al., 2021). Prior to multivariate analysis, data were auto scaled by mean-centering and dividing by the standard deviation of each variable. Partial least square - discriminant analysis (PLS-DA) was performed to compare the lipid profile of control and exposed cells, and to identify discriminant lipids based on the variable influence on the projection (VIP) parameter. The goodness of fit (R2) and the predictive ability of the model (Q2) were calculated to assess the quality of the multivariate approach. Volcano plots based on fold-change values > 1.5 and a significance threshold of $p < 0.05$ (Student *t*-test) were used to visualize the significance and magnitude of the changes.

3. Results

3.1. Cytotoxicity and ROS generation

Cell viability was assessed with two fluorescent reagents that estimate the metabolic activity (AB) and membrane impairment (CFDA-AM) of cells. The most cytotoxic compounds were halobenzoquinones (DBBQ, DCBQ), and DBHB, with EC_{50} values between 22 and 33 μg/mL. The remaining DBPs tested showed no cytotoxicity in JEG-3 cells at concentrations below 100 μg/mL (Table 1).

The generation of ROS was particularly high in cells exposed to 0.5–10 μg/mL halobenzoquinones (DBBQ and DCBQ), with up to 80-fold induction observed after 15 min of exposure to 10 μg/mL. Over the course of the 180-min exposure period, ROS generation gradually decreased by up to 50-fold (Fig. 1). Exposure of JEG-3 cells to halophenols (TBP, TCP; 5–10 μg/mL) resulted in an increase in ROS generation (1.5–2.5-fold). Similarly, DCSA, DBHBA and DCHBA caused a slight increase (up to 1.5-fold) in ROS (Fig. 1), while DBSA, DBHB and DCHB did not significantly increase ROS production.

3.2. Gene expression in JEG-3 cells

Halobenzoquinones were the compounds with the highest ability to up-regulate the expression of *cyp1a1* in JEG-3 cells after 24 h of exposure (up to 130-fold), far followed by DBHB (3-fold), DBSA (2.5-fold), DCHB (2-fold), and DCSA (1.5-fold) (Fig. 2A). The phenolic compounds (TBP, TCP) and halohydroxybenzoic acids (DBHBA, DCHBA) did not induce the expression of *cyp1a1* (Fig. 2A). Additionally, DBBQ and DCBQ significantly up-regulated the genes involved in estrogen synthesis in JEG-3 cells, with *cyp19a1* showing a 2-fold increase and *hsd17b12* exhibiting a 5-fold increase, whereas the expression of *hsd17b1* was up-regulated by the remaining compounds, reaching a maximum of 2.5-fold induction (Fig. 2B). An overview of the expression of all these genes in control JEG-3 cells is given in Fig. S1 (Supplementary info).

Table 1
Concentrations of 2,6-dichloro-1,4-benzoquinone (DCBQ), 2,6-dibromo-1,4-benzoquinone (DBBQ) and 3,5-dibromo-4-hydroxybenzaldehyde (DBHB) leading to a 50 % decrease in cell viability (EC_{50}) in JEG-3 cells after 24-h exposure. EC_{50} values are expressed as mean (μg/mL) ± SD of three independent experiments, six replicates each. No decrease in cell viability was detected for other compounds tested at a maximum concentration of 100 μg/mL. AB: Alamar Blue; CFDA-AM: 5-carboxyfluorescein diacetate acetoxymethyl ester.

Compound	EC_{50} (AB)	EC_{50} (CFDA-AM)
DCBQ	28.6 ± 2.79	26.2 ± 1.92
DBBQ	26.2 ± 1.61	22.2 ± 1.95
DBHB	26.0 ± 2.66	32.9 ± 0.71

3.3. Analysis of micronuclei in A549 cells

The genotoxic potential of haloaromatic DBPs was assessed by counting the micronuclei formed during the mitosis of exposed cells. The frequency of micronuclei induced by the positive control mitomycin (0.25 μM) was 28.4 ± 0.96 ‰, whereas control cells (0.1 % DMSO) had a micronuclei frequency of 1.84 ± 0.12 ‰ (for details see Table S2). Among the investigated DBPs, TBP and TCP showed significant genotoxicity when tested at a high concentration (100 μg/mL), inducing a frequency of micronuclei formation (29–31 ‰) comparable to that detected for mitomycin at a concentration 1000-fold lower. DBHB also induced the formation of micronuclei (17.5 ± 6.88 ‰) at the highest concentration tested (100 μg/mL) (Table S2).

3.4. Lipidome of JEG-3 cells

The lipidomic analysis identified 98 lipid species across 12 lipid subclasses, including cholesterol esters (CE), ceramides (Cer), DG, lysophosphatidylcholines (LPC), PC, PC-P, PE, phosphatidylglycerols (PG), PI, PS, sphingomyelins (SM), and TG in JEG-3 cells. The PLS-DA showed a segregation among lipid profiles of control cells and those exposed to the lowest concentration of DCBQ (0.5 μg/mL) (R2 = 0.951; Q2 = 0.659; 41.7 % covariance). The lipids responsible for this discrimination were mainly membrane lipids (up-regulation of PCs, PC-P/PC-Os, LPCs, SMs; down-regulation of PEs) (for details see Fig. S2). When cells were exposed at a higher concentration of DCBQ (1 μg/mL), and additional down-regulation of PIs was detected. In contrast, no clear discrimination between the lipidome of control and exposed cells was induced by exposure to the brominated analog (DBBQ) at 0.5 μg/mL, while a weak discrimination was evidenced at 1 μg/mL by PLS-DA (R2 = 0.906; Q2 = 0.005; 36.5 % covariance). Similarly to DCBQ, the discriminant lipids in the case of DBBQ were membrane lipids (up-regulation of PC-P/PC-Os, LPEs, SMs; down-regulation of PEs, PIs) (Fig. S2).

The univariate analysis confirms the findings of the PLS-DA and demonstrates a stronger impact of the chlorinated compound (DCBQ) compared to the brominated one (DBBQ) on the lipidome of placental cells. No significant changes were detected in the lipid composition of cells exposed to 0.5 μg/mL DBBQ. However, concentrations of 1 and 5 μg/mL DBBQ resulted in a decrease in certain species of PEs, PIs, and PSs, along with an increase in monounsaturated and/or saturated SMs, PC-Os, and LPCs (Fig. 3A and B). On the other hand, even at the low concentration of 0.5 μg/mL, the chlorinated compound DCBQ produced a similar but much stronger effect. The volcano plots highlighted a decrease in several species of PEs, as well as PIs and PSs, all of them mainly located in the inner part of the lipid bilayer. Like the brominated benzoquinone DBBQ, exposure to the chlorinated compound resulted in an increase of monounsaturated and saturated SMs, LPCs, and PC-Os even at the lowest concentrations tested (Fig. 3C, D and E).

4. Discussion

This study aimed to investigate the toxicological potential of haloaromatic byproducts formed during water disinfection, which are not currently regulated, but frequently detected at the ng/L to μg/L in disinfected waters (Kali et al., 2021; Yang et al., 2019). To address this research goal, we employed a battery of cell-based assays to evaluate various aspects, including cytotoxicity, generation of ROS, genotoxicity, ability to regulate the expression of steroidogenic genes, and potential to modulate the lipid composition of the cells.

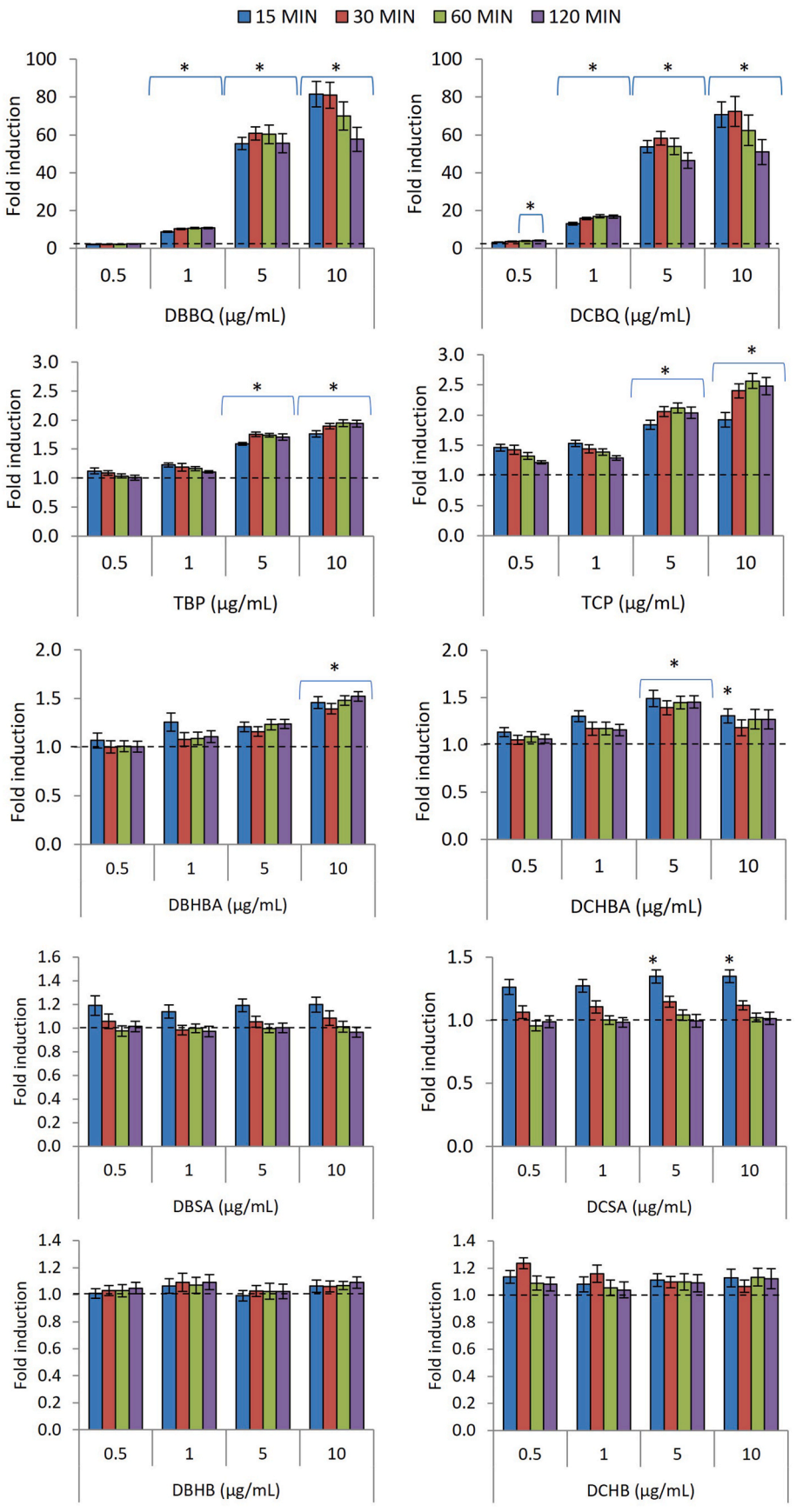

(caption on next page)

Fig. 1. Generation of reactive oxygen species (ROS) in JEG-3 cells after exposure to haloaromatic DBPs. Results are shown as fold induction over control cells, as mean ± SEM of at least three plates, each with 6 replicates. *Significant differences from control cells (dotted line). DBBQ: 2,6-dibromo-1,4-benzoquinone, DBHB: 3,5-dibromo-4-hydroxybenzaldehyde, DBHBA: 3,5-dibromo-4-hydroxybenzoic acid, DBSA: 3,5-dibromo-salicylic acid, DCBQ: 2,6-dichloro-1,4-benzoquinone, DCHB: 3,5-dichloro-4-hydroxybenzaldehyde, DCHBA: 3,5-dichloro-4-hydroxybenzoic acid, DCSA: 3,5-dichloro-salicylic acid, TBP: 2,4,6-tribromophenol, TCP: 2,4,6-trichlorophenol.

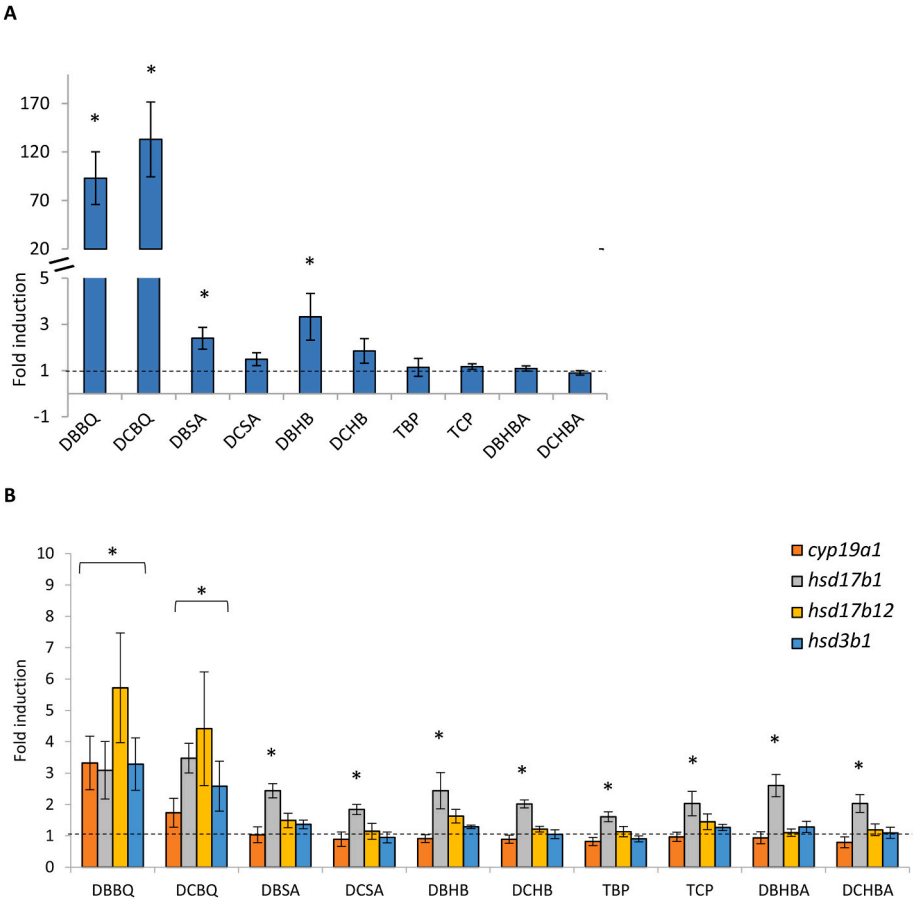

Fig. 2. Relative expression of (A) *cyp1a1*, and (B) genes involved in the biosynthesis of estrogens in JEG-3 cells exposed to 5 μg/mL of haloaromatic DBPs for 24 h. Results are expressed as fold induction ± SEM (n = 8). *Significant differences from control cells (dotted line). DBBQ: 2,6-dibromo-1,4-benzoquinone, DBHB: 3,5-dibromo-4-hydroxybenzaldehyde, DBHBA: 3,5-dibromo-4-hydroxybenzoic acid, DBSA: 3,5-dibromo-salicylic acid, DCBQ: 2,6-dichloro-1,4-benzoquinone, DCHB: 3,5-dichloro-4-hydroxybenzaldehyde, DCHBA: 3,5-dichloro-4-hydroxybenzoic acid, DCSA: 3,5-dichloro-salicylic acid, TBP: 2,4,6-tribromophenol, TCP: 2,4,6-trichlorophenol, *cyp19a1*: Cytochrome P450 family 19 subfamily A member 1, *hsd17b1*: hydroxysteroid 17-beta dehydrogenase 1, *hsd17b12*: hydroxysteroid 17-beta dehydrogenase 12, *hsd3b1*: hydroxy-delta-5-steroid dehydrogenase, 3 beta- and steroid delta-isomerase 1.

Among the 10 compounds tested, halobenzoquinones (DBBQ, DCBQ) and DBHB showed the highest cytotoxicity, with EC_{50} values ranging from 22 to 33 μg/mL, corresponding to 83–162 μM. These concentrations are five to six orders of magnitude higher than those commonly detected in swimming pool or tap water, respectively. Our findings are consistent with the cytotoxicity data obtained for halobenzoquinones in T24 bladder cancer cells after 24 h of exposure (EC_{50} values of 142 μM and 95 μM for DBBQ and DCBQ, respectively) (Li et al., 2014), although DBBQ was slightly more toxic than its chlorinated analogue in placental cells. On the other hand, the cytotoxicity of halobenzoquinones in CHO–K1 cells was significantly higher (EC_{50} values of 26 and 32 μM for DBBQ and DCBQ, respectively) compared to the placenta and bladder cell models, with the brominated analogue showing slightly higher toxicity than the chlorinated one. Interestingly, halobenzoquinones and DBHB were less toxic than bromoacetic acid and iodoacetic acid, but as toxic or even more toxic than other haloacetic acids, including the regulated CAA, in human placental cells (7.5 to > 250 μM) (Pérez-Albaladejo et al., 2023).

Oxidative stress has been identified as one of the main mechanisms of halobenzoquinones-induced cytotoxicity due to production of intracellular reactive oxygen species (ROS), depletion of the cellular antioxidant glutathione (GSH), inhibition of cellular antioxidant enzymes, and oxidative damage to DNA and proteins in Chinese hamster ovary (CHO–K1) cells (Li et al., 2014, 2016). Similarly, both DBBQ and DCBQ triggered a substantial increase in ROS production (80-fold) in human placental cells, significantly disrupting their cell redox status. In line with the cytotoxicity data, DCBQ induced more ROS formation in cells exposed at the lowest concentration (0.5 and 1 μg/L) compared to DBBQ. However, this trend shifted at the highest concentrations tested (5 and 10 μg/L). Trihalophenols (TBP, TCP) also showed a notable capacity to induce the generation of ROS (up to 2.5-fold).

Elevated ROS levels can damage components of cell membranes, including lipid bilayer, causing substantial alterations in membrane permeability and integrity, and consequently, compromising membrane functionality. Accordingly, the lipidomic analysis evidenced that exposure to halobenzoquinones resulted in the depletion of polyunsaturated lipid species that constitute the cytosolic part of the cell membranes, namely PIs, PEs, and PSs. It is known that oxygen radicals react with

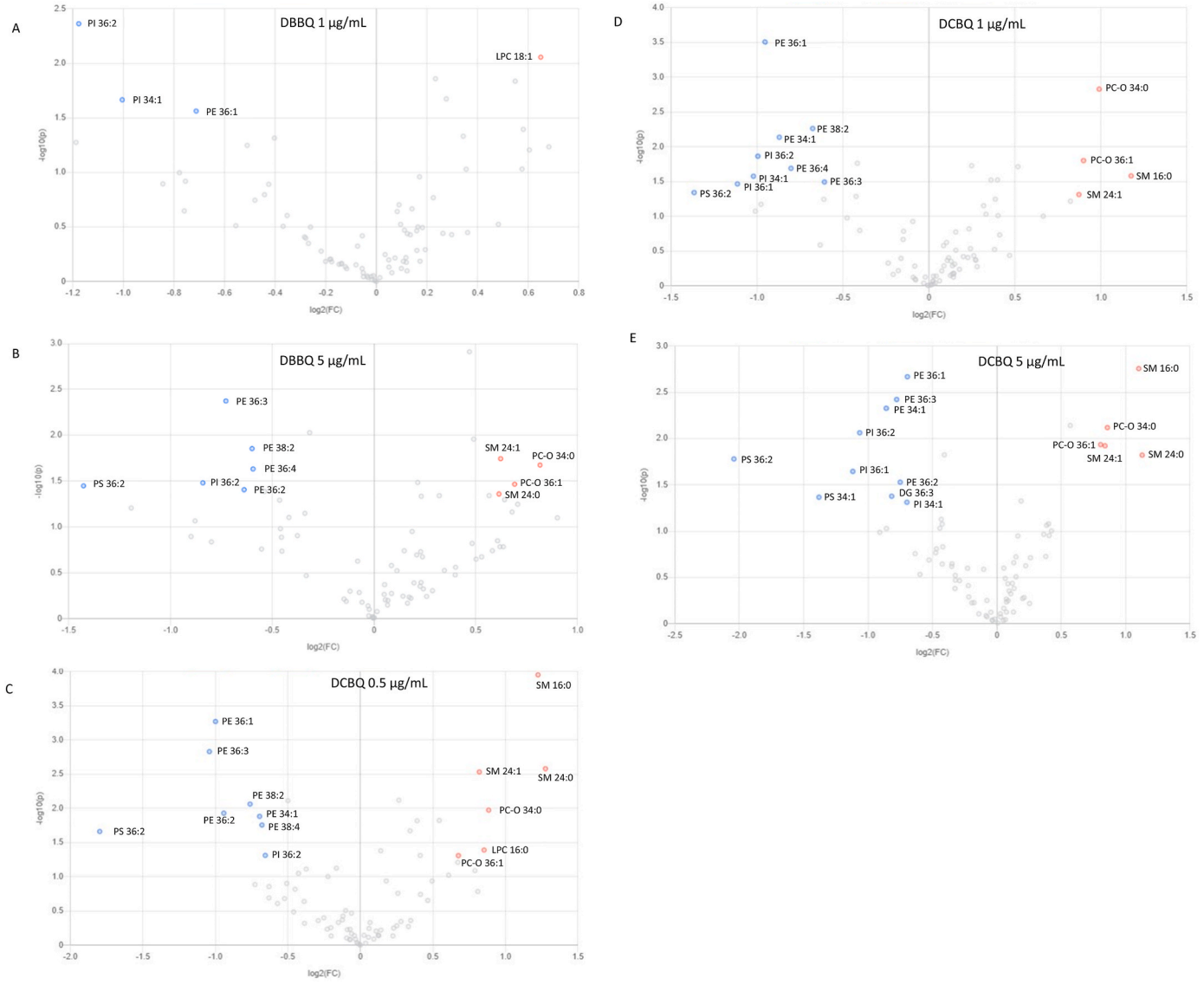

Fig. 3. Volcano plots that evidence differences in the lipid profile of JEG-3 cells exposed to various concentrations (0.5, 1 and 5 µg/ml) of the halobenzoquinones 2,6-dibromo-1,4-benzoquinone (DBBQ) (A, B) and 2,6-dichloro-1,4-benzoquinone (DCBQ) (C, D, E). Statistical significance (p-value; Student's t-test) and fold-change (FC) are plotted on the y and x axes, respectively. The lipids highlighted in red (up-regulated) or blue (down-regulated) are significantly different (FC $>$ 1.5; p $<$ 0.05). LPC: lyso-phosphatidylcholine; PC-O: phosphatidylcholine-plasmanyl, PE: phosphatidylethanolamine, PI: phosphatidylinositol, PS: phosphatidylserine, SM: sphingomyelin. (For interpretation of the references to colour in this figure legend, the reader is referred to the Web version of this article.)

lipids containing carbon-carbon double bonds, especially poly-unsaturated fatty acids that conform phospholipids (Martemucci et al., 2022). As a consequence, there was a significant decrease in PEs, PSs, and PIs containing 1 to 3 double bonds and 34 to 38 carbons, along with an increase in saturated and monounsaturated SMs (16:0, 24:0; 24:1) and ether-linked PCOs (34:0, 36:1). These alterations could be attributed to the excess of ROS generated by both DBBQ and DCBQ and the elevated susceptibility of double bonds to oxidative modification. But also, these changes suggest that exposure to halobenzoquinones has led to increased catabolism of PEs, probably to form PCs via the phosphatidylethanolamine N-methyltransferase (PEMT) pathway, and increased synthesis of SMs from PCs (Li et al., 2006). The consequences of these changes for placenta physiology are not yet fully undestood. It is important to note that SMs, PEs, PIs, and PSs are essential components of cell membranes, contributing both to the structure (membrane curvature, integrity, and fluidity) and function (cell signaling), and that changes in these lipids may affect membrane functionality. Thus, SM-rich microdomains have been implicated in chemoresistance. The balance Cer/SMs also plays a crucial role in regulating various inflammatory responses, and SMs are believed to be important for the activation of inflammatory cells (Taniguchi and Okazaki, 2021). It is also interesting to highlight that preeclampsia chorionic arteries exhibit a higher content of SM16:0, 18:0, C24:0 compared to normotensive arteries, and increased levels of SMs have been detected in both tissue and plasma during preeclampsia (Del Gaudio et al., 2020; Dobierzewska et al., 2017).

In addition to alterations in the lipidome, exposure to DBBQ and DCBQ resulted in a remarkable 100-fold induction in the expression of *cyp1a1*. This points to the activation of the aryl hydrocarbon receptor (AhR) by both halobenzoquinones, leading to increased expression of *cyp1a1,* which codifies for a CYP1A isoenzyme responsible for the oxidative metabolism of halobenzoquinones as well as a wide array of xenobiotics in placenta cells. In addition, both DBBQ and DCBQ were found to induce the expression of *cyp19a1* in placental cells, while the rest of DBPs investigated did not modulate the expression of this gene involved in the aromatization of androgens into estrogens. This contrasts

with a previous study by Koch and Sures (2018) that reported that 9 μM TBP (3 μg/mL) had the capacity to stimulate *cyp19a1* gene expression in H295 human placental cells. However, this effect was not detected in JEG-3 cells. Interestingly, in our study, not only halobenzoquinones, but the other investigated DBPs, up-regulated the expression *hsd17b1*, which encodes for a cytosolic enzyme that catalyzes the metabolism of estrone to estradiol. More recently, transcriptomic studies have revealed alterations in the expression of androgen and estrogen-related genes in HepG2 cells after exposure to halophenolic DBPs (Li et al., 2023). These findings collectively highlight the complex and multifaceted impact of DBPs on gene expression, particularly in the context of hormonal regulation. These effects were observed at concentrations that are not environmentally relevant. However, due to the continuous exposure to DBPs and the complex mixtures of often unknown byproducts/metabolites to which individuals are exposed, these findings should serve as a call to further investigate the potential role of DBPs, particularly DBBQ and DCBQ, as endocrine disruptors.

While oxidative stress has been proposed as a pivotal mechanism underlying the cytotoxicity and genotoxicity induced by quinones (Sheng and Lu, 2017), our study did not detect a significant increase in micronuclei formation in A549 cells. This may be attributed to the long exposure time (48 h) compared to the short half-life of halobenzoquinones in the culture medium (40 min in the case of DCBQ, as reported by Hung et al. (2019)). The instability of halobenzoquinones in culture medium may also have implications for the observed effects on cytotoxicity, lipid disruption and gene expression. Thus, the findings cannot be attributed exclusively to the tested halobenzoquinones but rather to their transformation byproducts, namely halo-hydroxyl-benzoquinones, which are stable in water and less toxic than halobenzoquinones (Wang et al., 2014).

In our study, trihalophenols were identified as the most genotoxic among the haloaromatic compounds tested, capable of inducing chromosomal damage and the formation of micronuclei in A549 lung cells after 48 h of exposure. However, these effects were observed at concentrations of 100 μg/mL (equivalent to 90 μM), significantly exceeding the concentrations of TBP detected in drinking water. Jansson and Jansson (1992) were the first to report the genotoxicity of TCP, observing 55 ‰ micronuclei formation in Chinese hamster V79 cells exposed for 24 h at 90 μg/mL. More recently, Liu et al. (2013) found a significant increase in micronucleus formation in erythrocytes of fish exposed to TCP over a period of 28 days. Both, TCP and TBP are widely used in various applications; for instance, TCP serves as an intermediate in the production of highly chlorinated phenols and is used as a preservative and pesticide, whereas TBP is used as a flame-retardant. Consequently, these chemicals may enter the environment, and organisms may be exposed through various sources beyond chlorinated water. Thus, TCP and TBP have been detected in wild organisms as well as in human blood and cord blood, at concentrations in the range of pg/g (Johnson et al., 2021; Koch and Sures, 2018). It is important to mention that these concentrations are below the levels that had a significant genotoxic effect in our study. Furthermore, it is worth noting the lower genotoxicity of haloaromatic DBPs in comparison to haloacetic acids, which induced the generation of micronuclei at 30 to 50-fold lower concentrations (Pérez-Albaladejo et al., 2023).

5. Conclusions

This study underscores the toxicological concern posed by halobenzoquinones in terms of generation of elevated ROS levels and significant alterations in placental cell lipid profiles, notably the loss of polyunsaturated lipid species. Although at concentrations in excess compared with the ones detected in swimming pool or tap water, all tested DBPs notably induced the expression of *hsd17b1*, potentially leading to an increased production estradiol. An estrogenic effect that was particularly prominent for halobenzoquinones, as they also induced an upregulation *cyp19a1* expression. Given that water disinfection yields a mixture of numerous DBPs at variable and generally low concentrations, further investigation into the synergistic effects of DBP mixtures is essential for a comprehensive understanding of DBP exposure and potential risks to organisms. Furthermore, as lifetime exposure of humans to these DBP mixtures may be significant, the assessment of chronic toxicity effects remains a critical area for future research. This study highlights the complexity of DBP toxicity and emphasizes the importance of continued investigation into their environmental and health implications.

CRediT authorship contribution statement

Elisabet Pérez-Albaladejo: Data curation, Investigation, Writing - original draft. **Marta Casado:** Methodology. **Cristina Postigo:** Conceptualization, Writing - review & editing. **Cinta Porte:** Conceptualization, Methodology, Supervision, Writing - review & editing.

Declaration of competing interest

The authors declare that they have no known competing financial interests or personal relationships that could have appeared to influence the work reported in this paper.

Data availability

Data will be made available on request.

Acknowledgments

CP acknowledges support from the Fundación General del CSIC through the ComFuturo Programme (2nd edition) and grant RYC2020-028901-I funded by MCIN/AEI/10.13039/501100011033 and "ESF investing in your future". This work was supported by "Agencia Estatal de Investigación" from the Spanish Ministry of Science and Innovation and the IDAEA-CSIC, a Centre of Excellence Severo Ochoa (CEX2018-000794-S) and project PID2021-122592NB-I00 (Ministerio de Ciencia e Innovación).

Appendix A. Supplementary data

Supplementary data to this article can be found online at https://doi.org/10.1016/j.envpol.2023.123092.

References

Barillet, S., Jugan, M.L., Laye, M., Leconte, Y., Herlin-Boime, N., Reynaud, C., Carrière, M., 2010. In vitro evaluation of SiC nanoparticles impact on A549 pulmonary cells: cyto-, genotoxicity and oxidative stress. Toxicol. Lett. 198, 324–330. https://doi.org/10.1016/j.toxlet.2010.07.009.

Chen, J., Thirkill, T.L., Lohstroh, P.N., Bielmeier, S.R., Narotsky, M.G., Best, D.S., Harrison, R.A., Natarajan, K., Pegram, R.A., Overstreet, J.W., Lasley, B.L., Douglas, G.C., 2004. Bromodichloromethane inhibits human placental trophoblast differentiation. Toxicol. Sci. 78, 166–174. https://doi.org/10.1093/TOXSCI/KFH046.

Colman, J., Rice, G.E., Wright, J.M., Hunter, E.S., Teuschler, L.K., Lipscomb, J.C., Hertzberg, R.C., Simmons, J.E., Fransen, M., Osier, M., Narotsky, M.G., 2011. Identification of developmentally toxic drinking water disinfection byproducts and evaluation of data relevant to mode of action. Toxicol. Appl. Pharmacol. 254, 100–126. https://doi.org/10.1016/J.TAAP.2011.02.002.

Del Gaudio, I., Sasset, L., Di Lorenzo, A., Wadsack, C., 2020. Sphingolipid signature of human feto-placental vasculature in preeclampsia. Int. J. Mol. Sci. 21, 1019. https://doi.org/10.3390/IJMS21031019, 2020.

Dobierzewska, A., Soman, S., Illanes, S.E., Morris, A.J., 2017. Plasma cross-gestational sphingolipidomic analyses reveal potential first trimester biomarkers of preeclampsia. PLoS One 12, e0175118. https://doi.org/10.1371/journal.pone.0175118.

Du, H., Li, J., Moe, B., McGuigan, C.F., Li, X.F., 2014. A real-time cell-electronic sensing method for comparative analysis of toxicity of water contaminants. Anal. Methods 6, 2053–2058. https://doi.org/10.1039/C3AY41686K.

Fenech, M., 2000. The in vitro micronucleus technique. Mutat. Res. Fund Mol. Mech. Mutagen 455, 81–95. https://doi.org/10.1016/S0027-5107(00)00065-8.

Fu, K.Z., Li, J., Vemula, S., Moe, B., Li, X.-F., 2017. Effects of halobenzoquinone and haloacetic acid water disinfection byproducts on human neural stem cells. J. Environ. Sci. 58, 239–249. https://doi.org/10.1016/j.jes.2017.02.006.

Grellier, J., Rushton, L., Briggs, D.J., Nieuwenhuijsen, M.J., 2015. Assessing the human health impacts of exposure to disinfection by-products - a critical review of concepts and methods. Environ. Int. 78, 61–81. https://doi.org/10.1016/j.envint.2015.02.003.

Han, J., Zhang, X., Jiang, J., Li, W., 2021. How much of the total organic halogen and developmental toxicity of chlorinated drinking water might Be attributed to aromatic halogenated DBPs? Environ. Sci. Technol. 55, 5906–5916. https://doi.org/10.1021/ACS.EST.0C08565.

Hu, S., Gong, T., Ma, J., Tao, Y., Xian, Q., 2018. Simultaneous determination of iodinated haloacetic acids and aromatic iodinated disinfection byproducts in waters with a new SPE-HPLC-MS/MS method. Chemosphere 198, 147–153. https://doi.org/10.1016/j.chemosphere.2018.01.124.

Hung, S., Mohan, A., Reckhow, D.A., Godri Pollitt, K.J., 2019. Assessment of the in vitro toxicity of the disinfection byproduct 2,6-dichloro-1,4-benzoquinone and its transformed derivatives. Chemosphere 234, 902–908. https://doi.org/10.1016/j.chemosphere.2019.06.086.

Jansson, K., Jansson, V., 1992. Genotoxicity of 2,4,6-trichlorophenol in V79 Chinese hamster cells. Mutat. Res. Genet. Toxicol. 280, 175–179. https://doi.org/10.1016/0165-1218(92)90046-3.

Jiang, J., Han, J., Zhang, X., 2020. Nonhalogenated aromatic DBPs in drinking water chlorination: a gap between NOM and halogenated aromatic DBPs. Environ. Sci. Technol. 54, 1646–1656. https://doi.org/10.1021/ACS.EST.9B06403/ASSET/IMAGES/LARGE/ES9B06403_0004.JPEG.

Johnson, C.L., Jazan, E., Kong, S.W., Pennell, K.D., 2021. A two-step gas chromatography-tandem mass spectrometry method for measurement of multiple environmental pollutants in human plasma. Environ. Sci. Pollut. Control Ser. 28, 3266–3279. https://doi.org/10.1007/s11356-020-10702-6.

Kali, S., Khan, M., Ghaffar, M.S., Rasheed, S., Waseem, A., Iqbal, M.M., Bilal khan Niazi, M., Zafar, M.I., 2021. Occurrence, influencing factors, toxicity, regulations, and abatement approaches for disinfection by-products in chlorinated drinking water: a comprehensive review. Environ. Pollut. 281, 116950 https://doi.org/10.1016/j.envpol.2021.116950.

Karahoda, R., Kallol, S., Groessl, M., Ontsouka, E., Anderle, P., Fluck, C., Staud, F., Albrecht, C., 2021. Revisiting steroidogenic pathways in the human placenta and primary human trophoblast cells. Int. J. Mol. Sci. https://doi.org/10.3390/ijms22041704.

Koch, C., Sures, B., 2018. Environmental concentrations and toxicology of 2,4,6-tribromophenol (TBP). Environ. Pollut. 233, 706–713. https://doi.org/10.1016/j.envpol.2017.10.127.

Li, J., Moe, B., Vemula, S., Wang, W., Li, X.-F., 2016. Emerging disinfection byproducts, halobenzoquinones: effects of isomeric structure and halogen substitution on cytotoxicity, formation of reactive oxygen species, and genotoxicity. Environ. Sci. Technol. 50, 6744–6752. https://doi.org/10.1021/acs.est.5b05585.

Li, J., Wang, W., Moe, B., Wang, H., Li, X.F., 2015. Chemical and toxicological characterization of halobenzoquinones, an emerging class of disinfection byproducts. Chem. Res. Toxicol. 28, 306–318. https://doi.org/10.1021/TX500494R.

Li, J., Wang, W., Zhang, H., Le, X.C., Li, X.-F., 2014. Glutathione-mediated detoxification of halobenzoquinone drinking water disinfection byproducts in T24 cells. Toxicol. Sci. 141, 335–343. https://doi.org/10.1093/toxsci/kfu088.

Li, X., Gao, X., Li, A., Xu, S., Zhou, Q., Zhang, L., Pan, Y., Shi, W., Song, M., Shi, P., 2023. Comparative cytotoxicity, endocrine-disrupting effects, oxidative stress of halophenolic disinfection byproducts and the underlying molecular mechanisms revealed by transcriptome analysis. Water Res. 229, 119458 https://doi.org/10.1016/J.WATRES.2022.119458.

Li, Z., Agellon, L.B., Allen, T.M., Umeda, M., Jewell, L., Mason, A., Vance, D.E., 2006. The ratio of phosphatidylcholine to phosphatidylethanolamine influences membrane integrity and steatohepatitis. Cell Metabol. 3, 321–331. https://doi.org/10.1016/J.CMET.2006.03.007.

Liu, J., Zhang, X., 2014. Comparative toxicity of new halophenolic DBPs in chlorinated saline wastewater effluents against a marine alga: halophenolic DBPs are generally more toxic than haloaliphatic ones. Water Res. 65, 64–72. https://doi.org/10.1016/j.watres.2014.07.024.

Liu, N., Ma, M., Xu, Y., Zha, J., Rao, K., Wang, Z., 2013. Susceptibility of male and female Japanese medaka (Oryzias latipes) to 2,4,6-trichlorophenol-induced micronuclei in peripheral erythrocytes. Front. Environ. Sci. Eng. 7, 77–84. https://doi.org/10.1007/s11783-012-0466-z.

Liu, X., Chen, L., Yang, M., Tan, C., Chu, W., 2020. The occurrence, characteristics, transformation and control of aromatic disinfection by-products: a review. Water Res. 184, 116076 https://doi.org/10.1016/J.WATRES.2020.116076.

Livak, K.J., Schmittgen, T.D., 2001. Analysis of relative gene expression data using real-time quantitative PCR and the 2−ΔΔCT method. Methods 25, 402–408. https://doi.org/10.1006/meth.2001.1262.

Lou, J., Wang, W., Lu, H., Wang, L., Zhu, L., 2021a. Increased disinfection byproducts in the air resulting from intensified disinfection during the COVID-19 pandemic. J. Hazard Mater. 418, 126249 https://doi.org/10.1016/J.JHAZMAT.2021.126249.

Lou, J., Wang, W., Zhu, L., 2021b. Transformation of emerging disinfection byproducts Halobenzoquinones to haloacetic acids during chlorination of drinking water. Chem. Eng. J. 418, 129326 https://doi.org/10.1016/j.cej.2021.129326.

Martemucci, G., Costagliola, C., Mariano, M., D'andrea, L., Napolitano, P., D'Alessandro, A.G., 2022. Free radical properties, source and targets, antioxidant consumption and health. Oxygen 2, 48–78. https://doi.org/10.3390/OXYGEN2020006.

Pang, Z., Chong, J., Zhou, G., De Lima Morais, D.A., Chang, L., Barrette, M., Gauthier, C., Jacques, P.É., Li, S., Xia, J., 2021. MetaboAnalyst 5.0: narrowing the gap between raw spectra and functional insights. Nucleic Acids Res. 49 https://doi.org/10.1093/nar/gkab382.

Pérez-Albaladejo, E., Lacorte, S., Porte, C., 2019. Differential toxicity of alkylphenols in JEG-3 human placental cells: alteration of P450 aromatase and cell lipid composition. Toxicol. Sci. 167, 336–346. https://doi.org/10.1093/toxsci/kfy243.

Pérez-Albaladejo, E., Pinteño, R., Aznar-Luque, M., del, C., Casado, M., Postigo, C., Porte, C., 2023. Genotoxicity and endocrine disruption potential of haloacetic acids in human placental and lung cells. Sci. Total Environ. 879 https://doi.org/10.1016/J.SCITOTENV.2023.162981.

Richardson, S.D., Plewa, M.J., Wagner, E.D., Schoeny, R., DeMarini, D.M., 2007. Occurrence, genotoxicity, and carcinogenicity of regulated and emerging disinfection by-products in drinking water: a review and roadmap for research. Mutat. Res. Rev. Mutat. Res. 636, 178–242. https://doi.org/10.1016/j.mrrev.2007.09.001.

Richardson, S.D., Postigo, C., 2015. Formation of DBPs: state of the science. ACS (Am. Chem. Soc.) Symp. Ser. https://doi.org/10.1021/bk-2015-1190.ch011.

Sheng, K., Lu, J., 2017. Typical airborne quinones modulate oxidative stress and cytokine expression in lung epithelial A549 cells. Journal of Environmental Science and Health, Part A 52, 127–134. https://doi.org/10.1080/10934529.2016.1237127.

Taniguchi, M., Okazaki, T., 2021. Role of ceramide/sphingomyelin (SM) balance regulated through "SM cycle" in cancer. Cell. Signal. 87, 110119 https://doi.org/10.1016/J.CELLSIG.2021.110119.

Tao, D., Wang, R., Shi, S., Yun, L., Tong, R., Peng, Y., Guo, W., Liu, Y., Hu, S., 2020. The identification of halogenated disinfection by-products in tap water using liquid chromatography–high resolution mass spectrometry. Sci. Total Environ. 740, 139888 https://doi.org/10.1016/j.scitotenv.2020.139888.

Villanueva, C.M., Kogevinas, M., Cordier, S., Templeton, M.R., Vermeulen, R., Nuckols, J.R., Nieuwenhuijsen, M.J., Levallois, P., 2014. Assessing exposure and health consequences of chemicals in drinking water: current state of knowledge and research needs. Environ. Health Perspect. 122, 213–221. https://doi.org/10.1289/ehp.1206229.

Wang, C., Yang, X., Zheng, Q., Moe, B., Li, X.F., 2018. Halobenzoquinone-induced developmental toxicity, oxidative stress, and apoptosis in zebrafish embryos. Environ. Sci. Technol. 52, 10590–10598. https://doi.org/10.1021/ACS.EST.8B02831.

Wang, W., Qian, Y., Li, J., Moe, B., Huang, R., Zhang, H., Hrudey, S.E., Li, X.F.X.-F., 2014. Analytical and toxicity characterization of halo-hydroxyl-benzoquinones as stable halobenzoquinone disinfection byproducts in treated water. Anal. Chem. 86, 4982–4988. https://doi.org/10.1021/ac5007238.

Yang, L., Chen, X., She, Q., Cao, G., Liu, Y., Chang, V.W.-C., Tang, C.Y., 2018. Regulation, formation, exposure, and treatment of disinfection by-products (DBPs) in swimming pool waters: a critical review. Environ. Int. 121, 1039–1057. https://doi.org/10.1016/j.envint.2018.10.024.

Yang, M., Zhang, X., Liang, Q., Yang, B., 2019. Application of (LC/)MS/MS precursor ion scan for evaluating the occurrence, formation and control of polar halogenated DBPs in disinfected waters: a review. Water Res. 158, 322–337. https://doi.org/10.1016/j.watres.2019.04.033.

Zhang, D., Bond, T., Krasner, S.W., Chu, W., Pan, Y., Xu, B., Yin, D., 2019. Trace determination and occurrence of eight chlorophenylacetonitriles: an emerging class of aromatic nitrogenous disinfection byproducts in drinking water. Chemosphere 220, 858–865. https://doi.org/10.1016/j.chemosphere.2018.12.127.

Zhang, D., Chu, W., Yu, Y., Krasner, S.W., Pan, Y., Shi, J., Yin, D., Gao, N., 2018. Occurrence and stability of chlorophenylacetonitriles: a new class of nitrogenous aromatic DBPs in chlorinated and chloraminated drinking waters. Environ. Sci. Technol. Lett. 5, 394–399. https://doi.org/10.1021/acs.estlett.8b00220.

Zhang, Z., Zhu, Q., Huang, C., Yang, M., Li, J., Chen, Y., Yang, B., Zhao, X., 2020. Comparative cytotoxicity of halogenated aromatic DBPs and implications of the corresponding developed QSAR model to toxicity mechanisms of those DBPs: binding interactions between aromatic DBPs and catalase play an important role. Water Res. 170, 115283 https://doi.org/10.1016/j.watres.2019.115283.